scientific reports

Check for updates

OPEN

Isotopic signatures and source apportionment of Pb in ambient $PM_{2.5}$

Chien-Cheng Jung[1], Charles C.-K. Chou[2]✉, Yi-Tang Huang[2], Shih-Yu Chang[3], Chung-Te Lee[4], Chuan-Yao Lin[2], Hing-Cho Cheung[2], Wei-Chen Kuo[5], Chih-Wei Chang[6] & Shuenn-Chin Chang[6,7]

Particulate lead (Pb) is a primary air pollutant that affects society because of its health impacts. This study investigates the source sectors of Pb associated with ambient fine particulate matter ($PM_{2.5}$) over central-western Taiwan (CWT) with new constraints on the Pb-isotopic composition. We demonstrate that the contribution of coal-fired facilities is overwhelming, which is estimated to reach 35 ± 16% in the summertime and is enhanced to 57 ± 24% during the winter monsoon seasons. Moreover, fossil-fuel vehicles remain a major source of atmospheric Pb, which accounts for 12 ± 5%, despite the current absence of a leaded gasoline supply. Significant seasonal and geographical variations in the Pb-isotopic composition are revealed, which suggest that the impact of East Asian (EA) pollution outflows is important in north CWT and drastically declines toward the south. We estimate the average contribution of EA outflows as accounting for 35 ± 15% (3.6 ± 1.5 ng/m^3) of the atmospheric Pb loading in CWT during the winter monsoon seasons.

Scientific studies have demonstrated that exposure to lead (Pb) particles is associated with hypertension[1,2]. It has also been indicated that a Pb level higher than 10 mg/dL in blood could result in a decline in the birth weight of infants[3] and intellectual impairment in children[4]. Studies have found that even low-level Pb exposure could cause damage to the nervous system[5,6] and hippocampus[7,8] and increase the risk of cognitive dysfunction[9]. The World Health Organization[10] recently published a report and indicated that Pb exposure was linked to irreversible neurological damage and caused 0.90 million deaths in 2019.

In the 1970s, Pb-alkyl additives in gasoline were a major source of Pb in the atmosphere[11,12]. Given the scientific evidence of the health impacts of lead exposure, the use of leaded fuels had been banned by some national governments in the 1980s and a worldwide phase-out was just announced by the United Nations Environment Programme (UNEP) recently. Consequently, a notable reduction in the ambient Pb level was achieved. For example, a study using reservoir sediment cores showed that the Pb level sharply declined from 1500 ng/m^3 in 1975 to 70 ng/m^3 in 1990 in the US[13], and some studies found decreases in ambient Pb level from 700 ng/m^3 in 1991 to 2.6 ng/m^3 in 2015 in Taipei, Taiwan[14–16]. However, elevated Pb levels have still been observed in recent studies in Taiwan, US, Czech, Poland, Saudi Arabia, and China, suggesting substantial air quality impacts of other sources[14,15,17–21]. Therefore, Pb remains a critical public health concern[22]. Investigations on the sources of Pb-containing particles have therefore been conducted, which have reported emissions of Pb stemming from a wide range of sources including but not limited to road dust, incinerators, coal-fired power plants, mines, bedrock, and construction work[23–29].

Because Pb-containing particles originating from various sources usually occur mixed in ambient fine particulate matter ($PM_{2.5}$), the identification and apportionment of sources of Pb particles is a highly challenging issue in air quality management. The positive matrix factorization (PMF) model is a statistical tool that is widely applied in air pollution investigations[14,29–31] and can resolve the contribution matrix of particulate matter pollution sources according to profiles of the chemical composition. However, the attribution of each factor to a specific pollution source is highly uncertain because the chemical profiles of pollution sources may exhibit common features[32]. Recently, scientists started to explore the isotopic characteristics of Pb collected from specific sources

[1]Department of Public Health, China Medical University, Taichung, Taiwan. [2]Research Center for Environmental Changes, Academia Sinica, Taipei, Taiwan. [3]Department of Public Health, Chung Shan Medical University, Taichung, Taiwan. [4]Graduate Institute of Environmental Engineering, National Central University, Taoyuan, Taiwan. [5]Meteorological Research Institute (MRI), Tsukuba, Japan. [6]Environmental Protection Administration, Taipei, Taiwan. [7]School of Public Health, National Defense Medical Center, Taipei, Taiwan. ✉email: ckchou@rcec.sinica.edu.tw

or ambient air[33–36] and, in turn, have assessed the impacts of various sources[15,27,37,38]. Studies have determined that the Pb isotopic composition changes due to variations in oil consumption and unleaded gasoline usage[39–42] and have suggested the major role of industrial emissions in present-day Pb pollution.

Taiwan is located offshore of southeastern China and is thus subject to the impacts of air pollution associated with East Asian (EA) continental outflows during the winter monsoon seasons. In addition, western Taiwan is a highly developed area with a population of approximately 23 million people and a large number of industrial factories, which emit a substantial amount of air pollutants. In this study, we present an in-depth analysis on two datasets, which were produced by the Taiwan EPA $PM_{2.5}$ speciation program in 2017–2019 and an intensive investigation conducted in the central-western Taiwan (CWT) from 2016 to 2018, respectively. Details of the two datasets are described in the section of Dataset and Method. We include the isotopic composition of Pb in the chemical profile of $PM_{2.5}$ samples and the Pb isotopic features of each pollution factor are then resolved with the PMF model, which adds new dimensions in source apportionment and helps to attribute Pb pollution to specific sources. Moreover, analysis of the geographical distribution of the Pb isotope ratios (i.e., $^{206}Pb/^{207}Pb$ and $^{208}Pb/^{207}Pb$) of $PM_{2.5}$ samples is conducted to investigate the influences of air pollution originating from local sources and/or transported by EA continental outflows during the winter monsoon seasons.

Results

Ambient concentration and mass mixing ratio of Pb in $PM_{2.5}$. This subsection presents analysis of the Pb content in the samples collected under the $PM_{2.5}$ speciation program of the Taiwan Environmental Protection Administration (EPA) during the period from 2017–2019. The average ambient concentration of Pb in $PM_{2.5}$ reached 7.9 ± 8.2, 8.3 ± 7.4 and 16.0 ± 22.1 ng/m^3 at the Zhongming (ZM), Douliu (DL), and Chiayi (CY) stations, respectively. The geographical locations of these sampling sites are shown in Supplementary Fig. 1. The results indicate that the Pb concentrations at Zhongming and Douliu are highly correlated ($r = 0.7386$), whereas the Pb concentration at Chiayi exhibits significantly different features ($p < 0.01$). In contrast, the corresponding $PM_{2.5}$ levels were 21.1 ± 11.5, 26.3 ± 14.3, and 26.5 ± 15.0 μg/m^3 at the three stations from 2017–2019. The $PM_{2.5}$ collected at Chiayi is characterized by an average Pb mass mixing ratio of 533 ± 613 ppm, which is 51% and 85% higher than the ratios of 354 ± 271 ppm and 289 ± 178 ppm, reported at the Zhongming and Douliu stations, respectively.

Figure 1 shows that both the ambient concentration and mass mixing ratio of Pb in $PM_{2.5}$ are associated with significant seasonal variations. The decline in the ambient Pb concentration in summer agrees with the typical air pollution pattern, which is usually the result of atmospheric dispersion enhancement[14,15]. However, the amplitude of the seasonal variation in the Pb concentration (i.e., winter mean/summer mean) ranges from 3.8–10.2 at the three sites, which is significantly larger than the amplitude of the variation in $PM_{2.5}$. The seasonal variation in the mass mixing ratio of Pb in $PM_{2.5}$ suggests that Pb more abundantly occurs in $PM_{2.5}$ during the period from September to April of the next year, which indicates that the sources of $PM_{2.5}$ could have changed with the seasons in CWT, and thereby merit an in-depth investigation.

Isotopic composition of Pb in $PM_{2.5}$. In order to facilitate investigation on the seasonal changes in the sources of Pb-containing particles in the CWT, Table 1 summarizes the isotopic composition of Pb in the $PM_{2.5}$ samples collected during the intensive investigation that was performed from 2016 to 2018. The overall average $PM_{2.5}$ concentrations was 23.5 ± 13.7 μg/m^3 in the study area, ranging from 20.0 ± 13.0 to 25.9 ± 17.0 μg/m^3 at the respective sites. The overall average ambient Pb concentration in $PM_{2.5}$ was 8.6 ± 7.2 ng/m^3, with the site-specific average concentrations ranging from 3.3 ± 2.2 to 15.6 ± 12.7 ng/m^3. While the overall average ambient Pb level during the sampling campaigns is comparable to the year round averages that reported in the previous subsection, this investigation reveals pronounced spatial differences in the ambient Pb concentration.

The overall average values of the $^{206}Pb/^{207}Pb$ and $^{208}Pb/^{207}Pb$ ratios were 1.148 ± 0.009 and 2.427 ± 0.012, respectively. Considering the potential seasonal changes in the sources of Pb in $PM_{2.5}$, the sampling campaigns were further divided into summer (i.e., August 2017 and July 2018) and winter (November 2016, February 2017 and March 2018) campaigns. The summer average values of $^{206}Pb/^{207}Pb$ and $^{208}Pb/^{207}Pb$ were 1.145 ± 0.010 and 2.419 ± 0.011, respectively, whereas the winter average values reached 1.150 ± 0.008 and 2.432 ± 0.011, respectively. Both isotopic ratios exhibited significant seasonal differences ($p < 0.01$). Figure 2 illustrates the correlation between $^{206}Pb/^{207}Pb$ and $^{208}Pb/^{207}Pb$. The two isotopic ratios maintained a significant linear correlation, whereas a steeper slope was associated with the winter dataset. A larger slope value indicates a significant increase in the relative abundance of ^{208}Pb during the winter monsoon seasons. Moreover, it should be noted that both $^{206}Pb/^{207}Pb$ and $^{208}Pb/^{207}Pb$ exhibited an increasing trend and moved toward the case representing EA continental outflows (as shown in Fig. 2) during the winter monsoon seasons.

Source identification of Pb in $PM_{2.5}$. To resolve the contribution of the pollution sources responsible for Pb in $PM_{2.5}$, this study employed the PMF model to analyze the data obtained during the intensive investigation. Note that the 3 Pb isotopes (^{206}Pb, ^{207}Pb, and ^{208}Pb) were independently considered in the chemical profiles, and the retrieved factors were in turn characterized based on Pb isotopic ratios (i.e., $^{206}Pb/^{207}Pb$ and $^{208}Pb/^{207}Pb$). PMF analysis provided a solution involving 8 factors. The chemical profiles of respective factors are illustrated in Supplementary Fig. 2. However, considering the uncertainties associated with the measurements and source apportionment, we examined only the top 4 factors in this study. Attribution of the source factors was based on the characteristic elements of the chemical profiles. In summary, the four major source factors of Pb included the following: (1) traffic emissions, (2) the petrol industry, (3) coal-fired facilities, and (4) oil-fired facilities. Notably, all four major sources were related to the production and/or use of fossil fuels. Table 2 summarizes the contribution of 4 major source factors to the total Pb in $PM_{2.5}$ in the study area and the Pb isotopic ratios

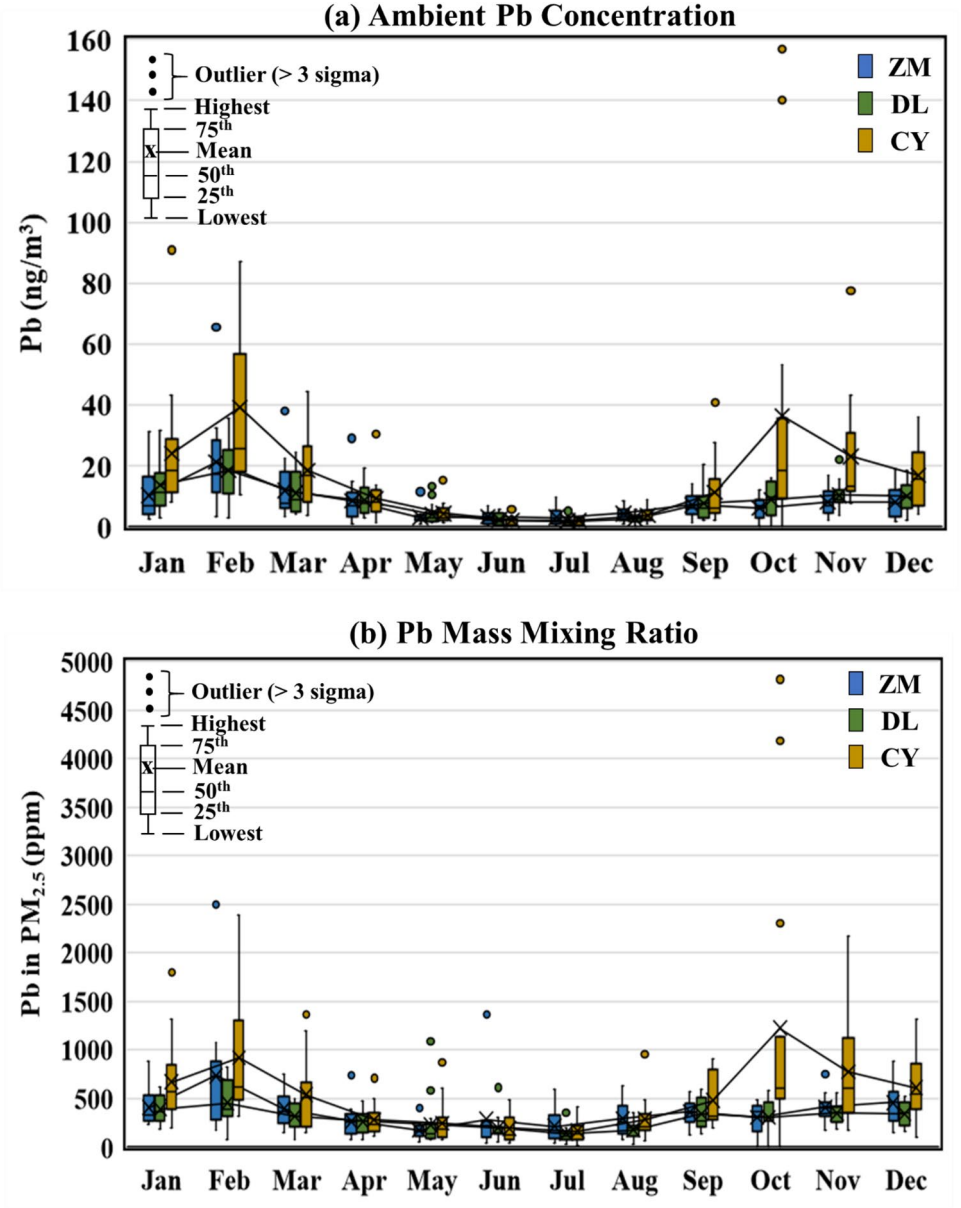

Figure 1. Seasonal variations in the ambient concentrations (**a**) and mass mixing ratios (**b**) of Pb in $PM_{2.5}$. Samples are collected at the Zhongming (ZM), Douliu (DL), and Chiayi (CY) sites of the Taiwan EPA $PM_{2.5}$ speciation network from 2017–2019. Geographic information on the sampling sites is shown in Supplementary Fig. 1.

and characteristic elements considered to achieve source attribution, whereas a summary of all the 8 factors is provided in Supplementary Table 3. In total, the top 4 factors accounted for ~ 80% of the total Pb in $PM_{2.5}$. Note that the above attribution of source factors resolved by the PMF model was based simply on the characteristic elements illustrated in the chemical profiles, but there could be contributions of unidentified minor sources not accounted for.

The contribution of traffic emissions (Factor 1) to Pb in $PM_{2.5}$ was estimated to reach 12 ± 5% in the study area despite the current lack of leaded gasoline usage. The attribution of this factor was based not only on the dominance of the variations in Cu, Mn and Zn in $PM_{2.5}$ but also on the Pb isotopic ratios. This factor was characterized by $^{206}Pb/^{207}Pb$ and $^{208}Pb/^{207}Pb$ ratios of 1.146 and 2.418, respectively. As shown in Fig. 2, the Pb isotopic features are consistent with the features of gasoline and diesel supplied in Taiwan[43].

The second source factor was attributed to the petrol industry due to the abundance of source-specific characteristic elements, in particular La, Ce, and Nd[44]. The contribution of this factor was estimated to reach 11 ± 4% throughout the entire study period, whereas a higher contribution (16 ± 8%) was observed in summer. This is justified by the geographic location of local sources in the study area. Several petroleum refining factories are located in southern Taiwan, which occurs upwind of our study sites during the summer monsoon seasons.

Sampling site	$PM_{2.5}$ (μg/m³)	Pb (ng/m³)	$^{206}Pb/^{207}Pb$	$^{208}Pb/^{207}Pb$
Changhua (CH)	22.6 ± 12.1	9.6 ± 7.1	1.149 ± 0.008	2.429 ± 0.012
Douliu (DL)	24.8 ± 15.4	9.3 ± 7.0	1.145 ± 0.011	2.426 ± 0.015
Dali (DA)	25.0 ± 11.8	5.0 ± 3.9	1.147 ± 0.008	2.426 ± 0.015
Fengyuan (FY)	23.1 ± 9.6	3.7 ± 1.6	1.151 ± 0.010	2.429 ± 0.013
Chiayi (CY)	25.9 ± 17.0	15.6 ± 12.7	1.146 ± 0.008	2.421 ± 0.007
Erlin (EL)	23.7 ± 14.5	10.1 ± 6.5	1.153 ± 0.008	2.430 ± 0.011
Shalu (SL)	24.4 ± 12.5	3.3 ± 2.2	1.137 ± 0.011	2.417 ± 0.013
Xianxi (XX)	24.2 ± 11.7	6.1 ± 4.1	1.152 ± 0.008	2.424 ± 0.010
Xingang (XG)	24.7 ± 15.9	10.1 ± 6.3	1.147 ± 0.008	2.429 ± 0.008
Zhushan (ZS)	22.2 ± 13.5	7.1 ± 5.9	1.146 ± 0.008	2.429 ± 0.010
Mailiao (ML)	21.8 ± 14.1	8.0 ± 5.7	1.149 ± 0.010	2.424 ± 0.013
Lunbei (LB)	25.0 ± 15.7	9.9 ± 6.1	1.149 ± 0.008	2.428 ± 0.013
Taixi (TX)	20.0 ± 13.0	6.9 ± 5.1	1.153 ± 0.010	2.432 ± 0.016
Overall	23.5 ± 13.7	8.6 ± 7.2	1.148 ± 0.009	2.427 ± 0.012

Table 1. Summary of the average concentrations of $PM_{2.5}$ and Pb associated with Pb-isotopic composition during the intensive field investigation.

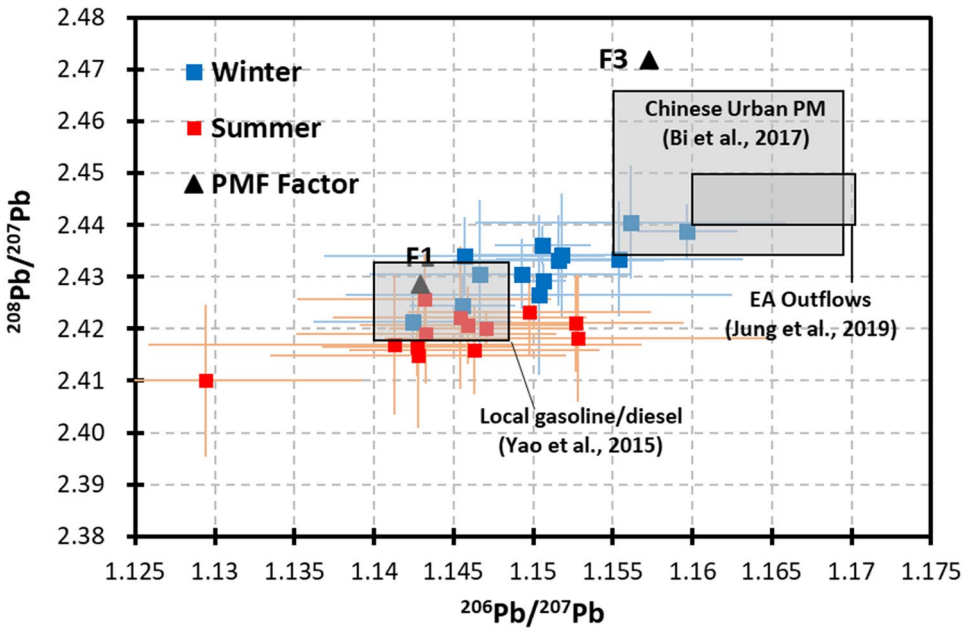

Figure 2. Distribution of the isotopic ratios of Pb in $PM_{2.5}$ in the summer and winter samples. Samples are collected at 13 sampling sites in central-western Taiwan during 5 field campaigns from 2016–2018, as described in the main text. The site-specific averages are denoted by symbols with ranges of ± 1 standard deviation, as shown by the error bars. The isotopic ratios of 2 PMF factors (F1 and F3) are denoted by triangles, whereas the other factors are beyond the ranges of this plot. The ranges of the isotopic ratios for fuels supplied in Taiwan, Chinese urban particulate matter and $PM_{2.5}$ transported by EA outflows are indicated with gray squares, with relevant references noted.

Coal-fired facilities (Factor 3) contributed almost half (49 ± 12%) of Pb in $PM_{2.5}$ in this area. This source factor exhibited significant seasonal differences, contributing 35 ± 16% to the Pb loading during the summer campaigns and 57 ± 24% during the winter campaigns on average. This factor was characterized by $^{206}Pb/^{207}Pb$ and $^{208}Pb/^{207}Pb$ ratios of 1.159 and 2.467, respectively. As shown in Fig. 2, this Pb isotopic feature is similar to that of aerosol samples collected in Chinese urban areas with significant pollution attributed to coal combustion[41]. It has been previously reported that the concentration and mixing ratio of Pb in $PM_{2.5}$ are enhanced during the EA winter monsoon seasons, suggesting influences of pollution transported from eastern and/or northern China. Here, the argument is further supported by Pb isotope evidence.

The 4th source factor encompassed oil-fired facilities because the variations in Ni and V in $PM_{2.5}$ were predominant. Given that residue oil is used mostly in heavy duty engines and boilers, this source was likely related

PMF factor (attribution)	Contribution, %*	$^{206}Pb/^{207}Pb$	$^{208}Pb/^{207}Pb$	Characteristic constituents#
F1 (traffic emissions)	12 ± 5 (S: 12 ± 6 W: 12 ± 7)	1.146 ± 0.005	2.418 ± 0.009	Zn (51%), Cu (31%), Mn (23%), Pb (12%) (Lin et al.[26])
F2 (petrol industry)	11 ± 4 (S: 16 ± 8 W: 8 ± 3)	1.148 ± 0.009	2.292 ± 0.008	Nd (56%), Ce (51%), Ti (48%), La (39%), Sr (26%) (Chow[55]; Kulkarni et al.[56]; Moreno et al.[57])
F3 (coal-fired facilities)	49 ± 12 (S: 35 ± 16 W: 57 ± 24)	1.159 ± 0.004	2.467 ± 0.006	Cd (57%), Pb (52%), As (40%), Se (32%) (Okuda et al.[58])
F4 (oil-fired facilities)	10 ± 5 (S: 21 ± 8 W: 6 ± 2)	1.126 ± 0.004	2.278 ± 0.005	V (65%), Ni (43%) (Querol et al.[59]; Cheng et al.[60])

Table 2. Summary of source apportionment for Pb in $PM_{2.5}$ and Pb isotopic composition of the respective source factors resolved by the PMF model. *Averages for summer (S) and winter (W) campaigns are listed in parentheses. #The percentage of variations in the characteristic elements attributed to each PMF factor is listed in parentheses.

to the emissions of ships and industrial facilities. This factor contributed 10 ± 5% to the Pb loading throughout the entire study period, whereas a significantly high contribution (21 ± 8%) was estimated during the summer campaigns. This seasonality was further justified by the geographic distribution of pollution sources in Taiwan. The majority of the heavy industry is located in southern Taiwan. Moreover, this factor could have been influenced by local circulation because sea breezes prevail in summer and thus could transport more ship emissions from the Taiwan Strait into the study area.

Discussion

Pb isotopic fingerprints of coal-fired facilities. The results in this study indicate that the ambient concentration and mass mixing ratio of Pb in $PM_{2.5}$ over CWT were significantly higher during the EA winter monsoon seasons than those during the summertime. Analysis of the back-trajectories of the air masses arriving in the study area on the sampling days reveals that Taiwan was influenced by EA outflows during the winter campaign periods and by southwesterlies during the summer campaign periods (as shown in Supplementary Fig. 4). PMF analysis determined the predominant factor of the contribution of coal-fired facilities (F3), which accounted for 57 ± 24% of the ambient Pb loading during the wintertime. Accordingly, it is plausible that the emission of Pb-containing particles by coal-fired facilities in China is a predominant source of atmospheric Pb in the CWT area during the wintertime. However, PMF analysis also determined a substantial contribution (35 ± 16%) of this factor (F3) during the summer campaigns, when Taiwan is typically impacted by southwesterly monsoons and isolated from the influences of Chinese air pollution. Thus, there could occur local coal-fired facilities possessing certain Pb isotope fingerprints, such as that of F3 ($^{206}Pb/^{207}Pb$: 1.159 ± 0.004, $^{208}Pb/^{207}Pb$: 2.467 ± 0.006). Within this context, an investigation of the Pb isotopic features of the coal used by local suspected facilities is warranted to identify the sources of atmospheric Pb in Taiwan.

Geographical distribution of the isotopic composition of Pb in $PM_{2.5}$. This study reveals significant spatial differences in the ambient Pb level among the sampling sites. Based on the previous section, the $PM_{2.5}$ samples collected at the Chiayi site are more enriched in Pb than those collected at the other sites. The results of our intensive investigation (as listed in Table 1) confirm the high Pb level at Chiayi and indicate lower Pb levels at the Fengyuan and Shalu sites. Figure 3 shows the changes in the average ambient Pb level and isotopic ratios at each sampling site with the latitude. It is apparent that the ambient Pb level increases from the northern to the southern parts of the study area, where Fengyuan and Chiayi are located at the northern and southern ends, respectively. The average Pb isotopic ratios ($^{206}Pb/^{207}Pb$ and $^{208}Pb/^{207}Pb$) of $PM_{2.5}$ at Chiayi are 1.142 ± 0.006 and 2.421 ± 0.006, respectively, and 1.153 ± 0.007 and 2.421 ± 0.009, respectively, during the winter and summer campaigns, respectively. In contrast to the general seasonal shift in the Pb isotopic ratios presented above and shown in Fig. 3b, the $^{208}Pb/^{207}Pb$ ratio at Chiayi does not significantly vary with the season. Given the high $^{208}Pb/^{207}Pb$ values associated with Chinese air pollutants, as shown in Fig. 2, the isotopic data suggest that the influences of EA outflows on the Pb level at Chiayi are relatively minor. In contrast, the average Pb isotopic ratios ($^{206}Pb/^{207}Pb$ and $^{208}Pb/^{207}Pb$) of $PM_{2.5}$ at Fengyuan during the winter campaigns are 1.160 ± 0.003 and 2.439 ± 0.005, respectively, which are comparable to the characteristics of the aerosols transported by EA outflows, as shown in Fig. 2. As a result, it is inferred that Fengyuan is significantly influenced by EA outflows during the EA winter monsoon seasons. Notably, the summer-campaign average values of the $^{206}Pb/^{207}Pb$ and $^{208}Pb/^{207}Pb$ ratios of $PM_{2.5}$ at Fengyuan shift to 1.143 ± 0.008 and 2.419 ± 0.010, respectively, which are consistent with the winter Pb isotopic features of $PM_{2.5}$ at Chiayi. These seasonal and geographical shifts in the Pb isotopic features suggest variations in the transport of air pollutants, which will be further elaborated in the following section.

Estimation of the contribution of EA outflows to local Pb loadings. Given the narrow range of $^{208}Pb/^{207}Pb$ during the summertime and the significant spatial and seasonal shifts, as shown in Fig. 3b, we employ a two-end-member model to estimate the contribution of EA outflows during the winter campaigns in this study. We assume that the overall average $^{208}Pb/^{207}Pb$ value over the summer campaigns, i.e., 2.419 ± 0.011,

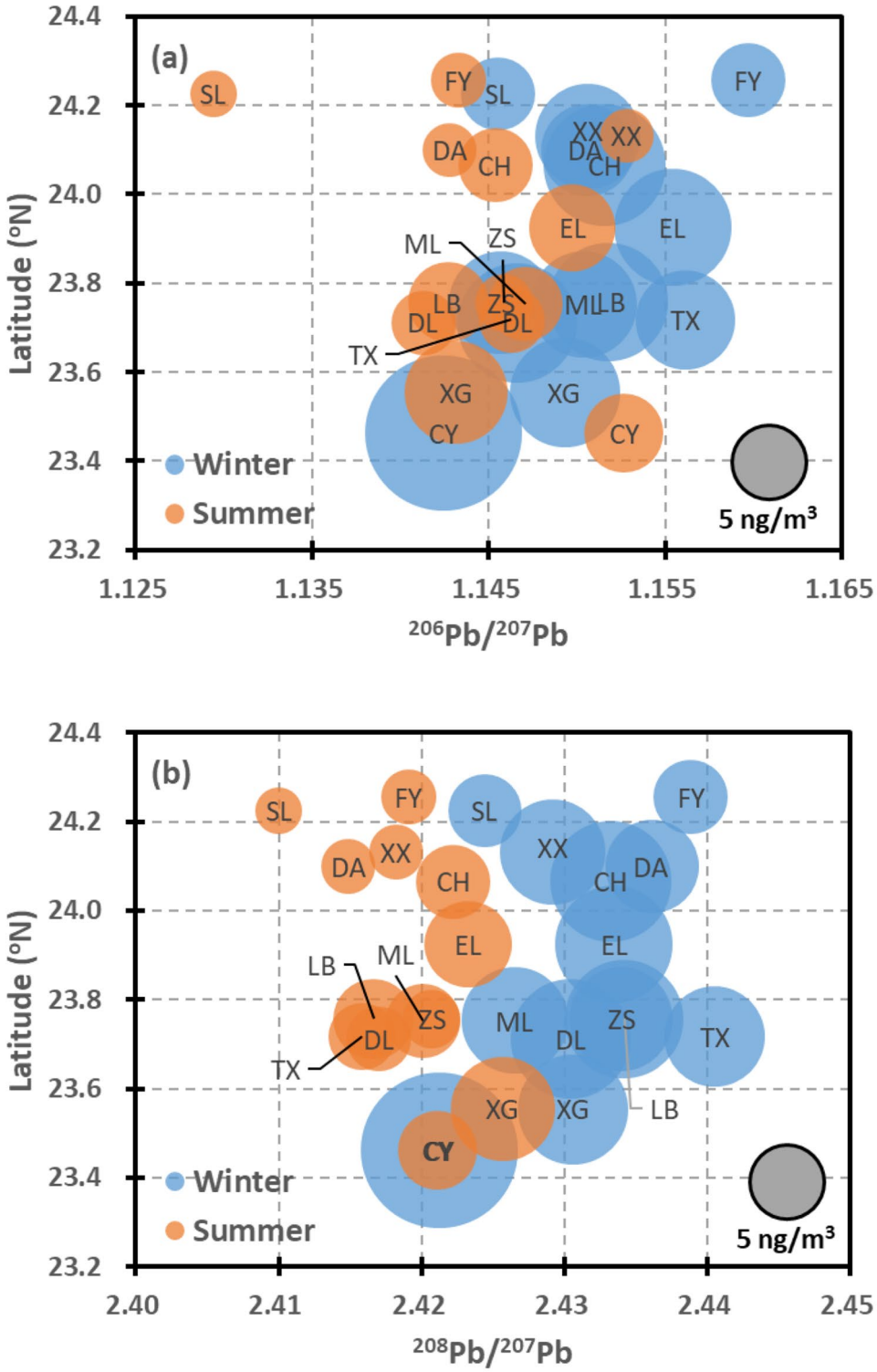

Figure 3. Geographical distribution of the ambient Pb levels and isotopic ratios, $^{206}Pb/^{207}Pb$ (**a**) and $^{208}Pb/^{207}Pb$ (**b**), along latitudes during the winter and summer campaigns. The circle area is proportional to the ambient mass concentration of Pb in $PM_{2.5}$. The coordinates of the respective sampling sites are listed in Supplementary Table 1, and labels of respective sites are **CH:** Changhua; **CY:** Chiayi; **DA:** Dali; **DL:** Douliu; **EL:** Erlin; **FY:** Fengyuan; **LB:** Lunbei; **ML:** Mailiao; **SL:** Shalu; **TX:** Taixi; **XG**: Xiangang; **XX:** Xianxi; **ZS:** Zhushan.

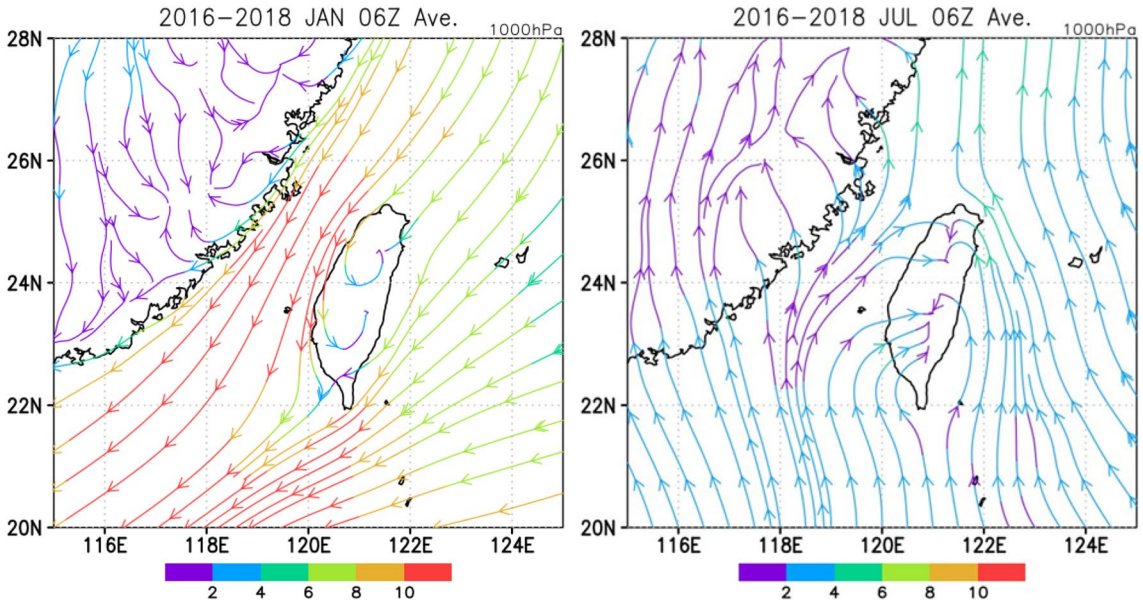

Figure 4. Mean surface streamlines in winter (January) and summer (July) from 2016–2018. The northeasterly East Asian winter monsoon branches reveal geographic blocking over Taiwan Island, which allows the development of side flows moving toward southeastern Taiwan. Weak southerly flows prevail during the summertime, and sea breezes dominate the transport of local air pollutants. The meteorological data at 06 UTC are used to demonstrate the general pattern of the wind field. The data are retrieved from the Global Data Assimilation System (GDAS).

represents the features of local pollution, while the average $^{208}Pb/^{207}Pb$ value based on Chinese urban measurements, as reported by Bi et al.[41], namely, 2.453 ± 0.009, represents the end member of EA outflows. Note that only the investigations conducted after 2000 are included here, considering the changes in pollution sources across China. As a result, it is estimated that EA outflows contribute $35 \pm 15\%$ or 3.6 ± 1.5 ng/m^3 to the ambient Pb loading over CWT during the winter monsoon seasons. The site-specific estimates are summarized in Supplementary Table 2. It should be noted that the influences of EA outflows are more pronounced along the western coastline and exhibit a declining trend toward the southern and inland (eastern) areas. There are two exceptional cases, namely, Shalu and Mailiao, where the $PM_{2.5}$ properties could have been dominated by specific sources located near these sampling sites.

Within the context of monsoon activity and the Pb isotopic features of $PM_{2.5}$ described above, the results in this study demonstrate that the influences of EA outflows could have drastically declined within only ~ 1 degree in latitude, i.e., from Fengyuan to Chiayi. This is explained by the development of local circulation in CWT. Figure 4 illustrates the mean surface (1000 hPa) streamlines around Taiwan calculated for January and July from 2016–2018, which represent the general transport patterns of air parcels in winter and summer, respectively. The streamlines indicate that the main stream of EA outflow is geographically blocked by the Central Mountain Ranges of Taiwan. As a result, a side flow moving toward southeastern Taiwan develops, particularly during the daytime. Consequently, the impacts of EA outflows diminish, and the pollutants emitted in the coastal areas of Taiwan could have dominated the air quality in the southern part of the study area. In contrast, the regional wind field is dominated by slow southerly flows during the summertime, and strong sea breezes could have driven local air pollutants eastward. The seasonal changes in local circulation suitably elucidate the geographical shift in the isotopic composition of Pb in $PM_{2.5}$.

Dataset and method

Datasets. Two datasets of Pb in $PM_{2.5}$ were analyzed and presented in this study. The first dataset is on the mass concentration of Pb measured at three sampling sites of Taiwan EPA during 2017–2019. The Taiwan EPA's sampling network comprises six stations distributed across Taiwan, and three of these six sites (Zhangming, Douliu, and Chiayi) are located within our study area. Geographic locations of the sampling sites are illustrated in the Supplementary Fig. 1. Under this program, each sample was collected over a 24-h period, and sampling was conducted regularly at 6-day intervals throughout the year. Thus, the advantage of this dataset is that it contains measurement for a whole year; it hence provides a more representative data of the ambient Pb level in the study area and a better picture for the spatial and seasonal variations in the ambient Pb concentration. Unfortunately, this program was initiated in 2017, and did not provide data for 2016. Moreover, the sampling sites were relatively sparse: only 3 sites located in our study area. The second dataset is the major dataset of this study, which is on the detailed chemical characterization of $PM_{2.5}$ samples collected from 13 sites during 5 sampling campaigns in 2016–2018, which is described in further details in the following. Geographic locations of the sampling sites are also illustrated in the Supplementary Fig. 1. The major advantage of this dataset is that it provides isotopic measurement of Pb for each $PM_{2.5}$ sample. However, because of the limited capacity of sampling/

analysis in lab, the sampling experiments were designed to investigate the winter/summer features and, thereby, did not provide a year-round seasonal variation. Moreover, we put more efforts to the spatial distribution and, thereby, only a limited number of samples were collected at each site.

Sample collection and chemical analysis of intensive investigation. An intensive investigation on the attribution of Pb in $PM_{2.5}$ was conducted in CWT from 2016–2018. A total of 274 daily $PM_{2.5}$ samples were collected at 13 sites distributed among urban, rural, and industrial zones across the study area during 5 sampling campaigns. $PM_{2.5}$ samples were simultaneously collected at the sites on a daily base for 7 to 10 days during each sampling campaign. Detailed information on the site categorization and sampling campaigns is provided in Supplementary Table 1.

At each sampling site, a BGI PQ200 sampler with airflow at 16.7 L/min (Mesa Labs, Inc., Butler, NJ, USA) was employed to collect $PM_{2.5}$ on Teflon filters, which were used for gravimetric measurement and analysis of crustal and metal elements (Al, As, Ca, Cd, Ce, Co, Cr, Cs, Cu, Fe, Ge, La, Mn, Mo, Nd, Ni, Pb, Rb, Sb, Se, Sn, Sr, Ti, Tl, V, Zn, Zr) and Pb isotopes (^{206}Pb, ^{207}Pb, and ^{208}Pb). In addition, a multichannel Super-SASS sampler with airflow at 6.7 L/min at each channel (Met One Instruments Inc., Grants Pass, OR, USA) was deployed to collect $PM_{2.5}$ on Teflon and tissue quartz-fiber filters. The Teflon filter samples were reserved for the analysis of soluble ions (Na^+, NH_4^+, K^+, Mg^{2+}, Ca^{2+}, Cl^-, NO_3^-, and SO_4^{2-}), whereas the quartz filter samples were reserved to determine the content of levoglucosan, organic carbon (OC) and elemental carbon (EC). To eliminate possible contamination, all quartz-fiber filters were pre-fired at 900 °C for 4 h before sampling.

The chemical analysis procedures for soluble ions, OC, EC, levoglucosan, and crustal/metal elements are described in previous publications[45–47]. In summary, each Teflon filter sample (from the Super-SASS device) was shaken with 10 mL deionized water for 60 min, and the extracts were then filtered. Ion chromatography (Dionex ICS-1100, Thermo Scientific) was conducted to analyze the soluble ions in the extracts. The OC and EC concentrations in the quartz filter samples (from the Super-SASS device) were determined with a DRI-2001A carbonaceous aerosol analyzer, following the IMPROVE-A thermo-optical reflectance (TOR) protocol. In addition, a punch (17 mm in diameter) of each quartz filter sample was extracted in 3 mL deionized water for 60 min, and an ion chromatography instrument equipped with a pulsed amperometric detector (PAD) (ICS-5000, Thermo Scientific) was then applied to analyze the content of levoglucosan in the extracts. The Teflon filter samples (from the PQ200 device) were completely dissolved in a mixture of acids in Teflon beakers, i.e., 4 mL HNO_3 (Merck LTD, 60% ultrapure) and 2 mL HF (Merck LTD, 48% ultrapure). An inductively coupled plasma-mass spectrometry (ICP-MS) instrument (NexION 300X, Perkin Elmer) was employed to determine the concentrations of crustal/metal elements in the digestion solutions. A fraction of each digestion solution was further purified with Sr-Spec resin (100–150 μm, Eichrom Technologies) in a cleanroom, which was in turn used to analyze Pb isotopes via ICP-MS[15]. The National Institute of Standards and Technology SRM 981 Pb standard was used to calibrate the Pb isotopic ratios.

Back-trajectory cluster analysis. Analysis of the 5-d back-trajectories of air masses was conducted twice per day using the Hybrid Single-Particle Lagrangian Integrated Trajectory (HYSPLIT) model of the National Oceanic and Atmospheric Administration (NOAA) on the sampling days. The meteorological data considered in the model included 6-hourly Global Data Assimilation System (GDAS) archived data with a resolution of 0.5 degrees in longitude and latitude. The end point of the trajectories occurred 200 m above ground level at the Dali station (24.02° N, 120.677° E), Taichung, Taiwan. Trajectory cluster analysis was then conducted to group trajectories into four clusters.

Positive matrix factorization (PMF) model. We used PMF 5.0 (from the US's Environmental Protection Administration) model to analyze the pollution source for ambient Pb. The basic principle of the PMF model was described in previous studies[48,49]. The mathematical expression of the PMF model is shown as Eq. (1):

$$\chi_{ij} = \sum_{k=1}^{p} g_{ik} f_{kj} + e_{ij} \tag{1}$$

where x_{ij} is the measured concentration of the jth species in the ith sample, p is a number of factor, g_{ik} is the contribution of the kth pollution source to the ith sample, f_{kj} is the concentration of the jth species from the kth pollution source, e_{ij} is the residual for each sample/species.

Because the results are constrained, no sample can have a negative source contribution. PMF allows each data point to be individually weighed. This feature allows the analyst to adjust the influence of each data point, depending on the confidence in the measurement. The PMF solution minimizes the object function Q based on the uncertainties (u) as Eq. (2):

$$\mathrm{Q(E)} = \sum_{i=1}^{n} \sum_{j=1}^{m} \left[\frac{X_{ij} - \sum_{k=1}^{p} g_{ijk_{ij}}}{u_{ij}} \right] \tag{2}$$

Where *uij* is the measured concentration (in μg/m^3) to the *jth* specie in *ith* sample, *n* is the number of samples, *m* is the number of species. The other parameters are the same as those in Eq. (1). The measured concentrations of $PM_{2.5}$ species were used here and the uncertainty is estimated using Eq. (3). In case with measured concentration of a specific species below method detection limit (MDL), a value of 50% MDL was used as input and the uncertainty is estimated using Eq. (4). We deployed measurements of 26 elements, 3 Pb isotopes (^{206}Pb, ^{207}Pb,

^{208}Pb), 7 ions, OC, EC, and levoglucosan to form the chemical profile in PMF. The novelty here is that the mass concentrations of the three isotopes of lead (^{206}Pb, ^{207}Pb, and ^{208}Pb) in $PM_{2.5}$ samples are measured and treated as 3 independent components in the chemical profile.

$$\text{Uncertainty} = \frac{5}{6} \times MDL \tag{3}$$

$$\text{Uncertainty} = \left[(\text{Error fraction} \times \text{concentration})^2 + (0.5 + \text{MDL})^2\right]^{1/2} \tag{4}$$

We used Eq. (5) to calculate the contribution of each pollution source to ambient Pb[50]:

$$R_{ij} = \sum_{k=1}^{n} g_{ik} f_{kj} / X_{ij} \tag{5}$$

where R_{ij} is the contribution of the jth species in the ith sample. The other parameters are the same as those in Eqs. 1 and 2. Then, the chemical profile of each contributing factor resolved by the PMF model contain the variance attributed to the 3 Pb-isotopes, respectively. Given the isotopic contribution, each contributing factor resolved in this study was further characterized by the ratios of Pb-isotopes (i.e. ^{206}Pb/^{207}Pb and ^{208}Pb/^{207}Pb).

We also deployed classical Bootstrap procedure to assess the uncertainty for PMF analysis[51,52]. In this study, the number of Bootstrap was assigned at 200 to run uncertainty assessment [51,53]. If the Bootstrap factor was not correlated with any base factors, the Bootstrap factor was classified as "unmapped"[54]. The detailed results of Bootstrap are described in the Supplementary Fig. 3. The Bootstrap analysis showed that most species, in particular the characteristic constituents for each factor, were contained in the IQR of variance, which suggested that results in base run were robust and representative.

Two-end-member model. This study used a two end-member model[37] to calculate the contributions of local source and the East-Asian outflows to the ambient Pb in $PM_{2.5}$ in the CWT following the Eq. (6):

$$\mathrm{R} = \mathrm{R_{EA}} \times f_{EA} + \mathrm{R_{LC}} \times \left(1 - f_{EA}\right). \tag{6}$$

where R is the measured Pb isotope ratio (i.e. ^{206}Pb/^{207}Pb or ^{208}Pb/^{207}Pb) of a $PM_{2.5}$ sample; R_{LC} and R_{EA} are respectively the Pb isotope ratios of the two end members: the local sources and the East-Asian outflows. In this study, the local end member is characterized by the measurements taken in summertime when Taiwan is isolated from the continental air mass, and the East-Asian end member is characterized by the measurements taken in polluted urban areas in China[41]. f_{EA} denotes the relative contribution of East-Asian outflows to ambient Pb, and $(1—f_{EA})$ is the relative contribution of local sources. Then, we separately calculate the relative contributions of local sources and EA outflows to ambient Pb for all sampling sites using ^{206}Pb/^{207}Pb and ^{208}Pb/^{207}Pb. Note that the results presented here are based on the analysis of ^{208}Pb/^{207}Pb because it exhibits a more distinct seasonality than is the ^{206}Pb/^{207}Pb, and thereby more suitable to this study.

Statistical analysis. A paired two-tailed t-test and analysis of variance was performed to investigate the differences in the chemical composition of $PM_{2.5}$ between the seasons and sampling sites, respectively. SAS 9.4 (SAS Institute Inc., Cary, NC, USA) statistical software was employed to analyze all data. Statistical significance was defined at $p < 0.05$.

Data availability

The data that support the findings of this study are available from the corresponding author upon reasonable request.

Received: 8 October 2021; Accepted: 2 March 2022
Published online: 14 March 2022

References

1. Schwartz, J. Lead, blood pressure, and cardiovascular disease in men. *Arch. Environ. Health: Int. J.* **50**, 31–37 (1995).
2. Sharp, D. S., Becker, C. E. & Smith, A. H. Chronic low-level lead exposure. *Med. Toxicol. Adverse Drug Exp.* **2**, 210–232 (1987).
3. Needleman, H. L., Rabinowitz, M., Leviton, A., Linn, S. & Schoenbaum, S. The relationship between prenatal exposure to lead and congenital anomalies. *JAMA* **251**, 2956–2959 (1984).
4. Canfield, R. L. *et al.* Intellectual impairment in children with blood lead concentrations below 10 μg per deciliter. *N. Engl. J. Med.* **348**, 1517–1526 (2003).
5. Finkelstein, Y., Markowitz, M. E. & Rosen, J. F. Low-level lead-induced neurotoxicity in children: an update on central nervous system effects. *Brain Res. Rev.* **27**, 168–176 (1998).
6. Mason, L. H., Harp, J. P. & Han, D. Y. Pb neurotoxicity: Neuropsychological effects of lead toxicity. *BioMed Res. Int.* **2014**, 1 (2014).
7. Jett, D. A., Kuhlmann, A. C., Farmer, S. J. & Guilarte, T. R. Age-dependent effects of developmental lead exposure on performance in the Morris water maze. *Pharmacol. Biochem. Behav.* **57**, 271–279 (1997).
8. Slomianka, L., Rungby, J., West, M., Danscher, G. & Andersen, A. Dose-dependent bimodal effect of low-level lead exposure on the developing hippocampal region of the rat: A volumetric study. *Neurotoxicology* **10**, 177–190 (1989).
9. Farooqui, Z. *et al.* Associations of cumulative Pb exposure and longitudinal changes in Mini-Mental Status Exam scores, global cognition and domains of cognition: The VA Normative Aging Study. *Environ. Res.* **152**, 102–108 (2017).
10. World Health Organization. Exposure to lead: a major public health concern, 2nd edition. (ed 2) (2021).
11. Mielke, H. W. & Zahran, S. The urban rise and fall of air lead (Pb) and the latent surge and retreat of societal violence. *Environ. Int.* **43**, 48–55 (2012).

12. Patterson, C. An alternative perspective-lead pollution in the human environment: origin, extent, and significance. *Lead Hum. Environ.* **1**, 265–349 (1980).
13. Callender, E. & Metre, P. C. V. Environmental policy analysis, peer reviewed: Reservoir sediment cores show US lead declines. *Environ. Sci. Technol.* **31**, 424A-428A (1997).
14. Hsu, C.-Y. *et al.* Elemental characterization and source apportionment of PM10 and PM25 in the western coastal area of central Taiwan. *Sci Tot Environ* **541**, 1139–1150 (2016).
15. Jung C-C, *et al.* C-Sr-Pb isotopic characteristics of PM2.5 transported on the East-Asian continental outflows. *Atmos. Res.* (2019).
16. Mao, I. & Chen, M. Airborne lead pollution in metropolitan Taipei (Republic of China). *Water Air Soil Pollut.* **91**, 375–382 (1996).
17. Tunno, B. J. *et al.* Indoor source apportionment in urban communities near industrial sites. *Atmos. Environ.* **139**, 30–36 (2016).
18. Schwarz, J. *et al.* PM2. 5 chemical composition at a rural background site in Central Europe, including correlation and air mass back trajectory analysis. *Atmos. Res.* **176**, 108–120 (2016).
19. PMF source attribution. Samek L, *et al.* Seasonal variations of chemical composition of PM2. 5 fraction in the urban area of Krakow, Poland. *Air Qual. Atmos. Health* **13**, 89–96 (2020).
20. Nayebare, S. R. *et al.* Chemical characterization and source apportionment of PM2 5 in Rabigh, Saudi Arabia. *Aerosol. Air Qual. Res.* **16**, 3114–3129 (2016).
21. Zhang, R. *et al.* Reconstruction of historical lead contamination and sources in Lake Hailing, Eastern China: a Pb isotope study. *Environ. Sci. Pollut. Res.* **23**, 9183–9191 (2016).
22. O'Connor, D. *et al.* Lead-based paint remains a major public health concern: a critical review of global production, trade, use, exposure, health risk, and implications. *Environ. Int.* **121**, 85–101 (2018).
23. Birmili, W., Allen, A. G., Bary, F. & Harrison, R. M. Trace metal concentrations and water solubility in size-fractionated atmospheric particles and influence of road traffic. *Environ. Sci. Technol.* **40**, 1144–1153 (2006).
24. Christian, T. J. *et al.* Trace gas and particle emissions from domestic and industrial biofuel use and garbage burning in central Mexico. *Atmos. Chem. Phys.* **10**, 565–584 (2010).
25. Hu, C.-W. *et al.* Characterization of multiple airborne particulate metals in the surroundings of a municipal waste incinerator in Taiwan. *Atmos. Environ.* **37**, 2845–2852 (2003).
26. Lin, Y.-C. *et al.* Characteristics of trace metals in traffic-derived particles in Hsuehshan Tunnel, Taiwan: Size distribution, potential source, and fingerprinting metal ratio. *Atmos. Chem. Phys.* **15**, 4117–4130 (2015).
27. Salcedo, D. *et al.* Using trace element content and lead isotopic composition to assess sources of PM in Tijuana, Mexico. *Atmos. Environ.* **132**, 171–178 (2016).
28. Wang, C.-F., Chang, C.-Y., Tsai, S.-F. & Chiang, H.-L. Characteristics of road dust from different sampling sites in northern Taiwan. *J. Air Waste Manag. Assoc.* **55**, 1236–1244 (2005).
29. Wang, S. *et al.* Source apportionment of metal elements in PM2. 5 in a coastal city in Southeast China: Combined Pb-Sr-Nd isotopes with PMF method. *Atmos. Environ.* **198**, 302–312 (2019).
30. Song, Y. *et al.* Source apportionment of PM2. 5 in Beijing by positive matrix factorization. *Atmos. Environ.* **40**, 1526–1537 (2006).
31. Ho, W.-Y., Tseng, K.-H., Liou, M.-L., Chan, C.-C. & Wang, C.-H. Application of positive matrix factorization in the identification of the sources of PM2. 5 in Taipei City. *Int. J. Environ. Res. Publ. Health* **15**, 1305 (2018).
32. Samek, L., Stegowski, Z. & Furman, L. Preliminary PM2. 5 and PM10 fractions source apportionment complemented by statistical accuracy determination. *Nukleonika* **61**, 75–83 (2016).
33. Widory, D., Liu, X. & Dong, S. Isotopes as tracers of sources of lead and strontium in aerosols (TSP & PM 2.5) in Beijing. *Atmos. Environ.* **44**, 3679–3687 (2010).
34. Widory, D. *et al.* The origin of atmospheric particles in Paris: a view through carbon and lead isotopes. *Atmos. Environ.* **38**, 953–961 (2004).
35. Souto-Oliveira, C., Babinski, M., Araújo, D., Weiss, D. & Ruiz, I. Multi-isotope approach of Pb, Cu and Zn in urban aerosols and anthropogenic sources improves tracing of the atmospheric pollutant sources in megacities. *Atmos. Environ.* **198**, 427–437 (2019).
36. Dong, S. *et al.* Isotopic signatures suggest important contributions from recycled gasoline, road dust and non-exhaust traffic sources for copper, zinc and lead in PM10 in London, United Kingdom. *Atmos. Environ.* **165**, 88–98 (2017).
37. Hsu, S.-C. *et al.* Lead isotope ratios in ambient aerosols from Taipei, Taiwan: Identifying long-range transport of airborne Pb from the Yangtze Delta. *Atmos. Environ.* **40**, 5393–5404 (2006).
38. Graney, J. R., Edgerton, E. S. & Landis, M. S. Using Pb isotope ratios of particulate matter and epiphytic lichens from the Athabasca Oil Sands Region in Alberta, Canada to quantify local, regional, and global Pb source contributions. *Sci. Total Environ.* **654**, 1293–1304 (2019).
39. Komárek, M., Ettler, V., Chrastný, V. & Mihaljevič, M. Lead isotopes in environmental sciences: a review. *Environ. Int.* **34**, 562–577 (2008).
40. Monna, F., Lancelot, J., Croudace, I. W., Cundy, A. B. & Lewis, J. T. Pb isotopic composition of airborne particulate material from France and the southern United Kingdom: implications for Pb pollution sources in urban areas. *Environ. Sci. Technol.* **31**, 2277–2286 (1997).
41. Bi, X.-Y. *et al.* Lead isotopic compositions of selected coals, Pb/Zn ores and fuels in China and the application for source tracing. *Environ. Sci. Technol.* **51**, 13502–13508 (2017).
42. Chou, C. K. *et al.* Seasonality of the mass concentration and chemical composition of aerosols around an urbanized basin in East Asia. *J. Geophys. Res.: Atmos.* **122**, 2026–2042 (2017).
43. Yao, P.-H. *et al.* Lead isotope characterization of petroleum fuels in Taipei, Taiwan. *Int. J. Environ. Res. Publ. Health* **12**, 4602–4616 (2015).
44. Chou, C. K. Development and application of carbon and lead isotopes analysis technology in fine particles). *Environ. Prot. Admin.* **1**, 1 (2014).
45. Chang, S.-Y., Fang, G.-C., Chou, C.C.-K. & Chen, W.-N. Source identifications of PM10 aerosols depending on hourly measurements of soluble components characterization among different events in Taipei Basin during spring season of 2004. *Chemosphere* **65**, 792–801 (2006).
46. Chou, C.-K. *et al.* Seasonal variation and spatial distribution of carbonaceous aerosols in Taiwan. *Atmos. Chem. Phys.* **10**, 9563–9578 (2010).
47. Lin, Y.-C. *et al.* Wintertime haze deterioration in Beijing by industrial pollution deduced from trace metal fingerprints and enhanced health risk by heavy metals. *Environ. Pollut.* **208**, 284–293 (2016).
48. Paatero, P. & Tapper, U. Positive matrix factorization: A non-negative factor model with optimal utilization of error estimates of data values. *Environmetrics* **5**, 111–126 (1994).
49. U.S.EPA. EPA Positive Matrix Factorization (PMF) 5.0 Fundamentals and User Guide.). U.S. Environmental Protection Agency (2014).
50. Wang, X. *et al.* Combining positive matrix factorization and radiocarbon measurements for source apportionment of PM 25 from a National Background Site in North China. *Sci. Rep.* **7**, 10648 (2017).
51. Men, C. *et al.* Uncertainty analysis in source apportionment of heavy metals in road dust based on positive matrix factorization model and geographic information system. *Sci. Total Environ.* **652**, 27–39 (2019).
52. Vlachou, A. *et al.* Development of a versatile source apportionment analysis based on positive matrix factorization: A case study of the seasonal variation of organic aerosol sources in Estonia. *Atmos. Chem. Phys.* **19**, 7279–7295 (2019).

53. Dvorská, A., Komprdová, K., Lammel, G., Klánová, J. & Plachá, H. Polycyclic aromatic hydrocarbons in background air in central Europe–seasonal levels and limitations for source apportionment. *Atmos. Environ.* **46**, 147–154 (2012).
54. Kioumourtzoglou, M.-A. *et al.* Exposure measurement error in PM 25 health effects studies: A pooled analysis of eight personal exposure validation studies. *Environ. Health* **13**, 1–11 (2014).
55. Chow, J. C. *et al.* Source profiles for industrial, mobile, and area sources in the Big Bend Regional Aerosol Visibility and Observational study. *Chemosphere* **54**, 185–208 (2004).
56. Kulkarni, P., Chellam, S. & Fraser, M. P. Tracking petroleum refinery emission events using lanthanum and lanthanides as elemental markers for PM2.5. *Environ. Sci. Technol.* **41**, 6748–6754 (2007).
57. Moreno, T., Querol, X., Alastuey, A. & Gibbons, W. Identification of FCC refinery atmospheric pollution events using lanthanoid- and vanadium-bearing aerosols. *Atmos. Environ.* **42**, 7851–7861 (2008).
58. Okuda, T. *et al.* Trends in hazardous trace metal concentrations in aerosols collected in Beijing, China from 2001 to 2006. *Chemosphere* **72**, 917–924 (2008).
59. Querol, X. *et al.* Source origin of trace elements in PM from regional background, urban and industrial sites of Spain. *Atmos. Environ.* **41**, 7219–7231 (2007).
60. Cheng, M.-T. *et al.* Chemical compositions of fine particulates emitted from oil-fired boilers. *J. Environ. Eng. Manag.* **18**, 355–362 (2008).

Acknowledgements

This study received financial support from the Taiwan Environmental Protection Administration under grants EPA-105-U101-02-A272, EPA-105-U102-03-A284, EPA-107-L101-02-A024 and EPA-107-L102-02-A038, the Ministry of Science and Technology under grants 105-2111-M-001-005-MY3 and 106-3114-M-001-001-A, and the Academia Sinica Grand Challenge Program AS-GC-110-01. The authors gratefully acknowledge the logistical support received at the respective sampling sites during the intensive field campaigns.

Author contributions

C.C.K.C. and S.C.C. conceived the Pb isotope research project. C.T.L. and S.C.C. organized the $PM_{2.5}$ speciation network in Taiwan. C.C.K.C. and C.C.J. led the team in data analysis. Y.T.H., S.Y.C. and C.W.C. organized the sampling program. Y.T.H. led the sample collection and chemical analysis. C.Y.L. conducted the streamline analysis. H.C.C. and W.C.K. contributed to cluster analysis of the back-trajectories. C.C.J. and C.C.K.C. wrote the manuscript with contributions from all coauthors.

Competing interests

The authors declare no competing interests.

Additional information

Supplementary Information The online version contains supplementary material available at https://doi.org/10.1038/s41598-022-08096-1.

Correspondence and requests for materials should be addressed to C.C.-K.C.

Reprints and permissions information is available at www.nature.com/reprints.

Publisher's note Springer Nature remains neutral with regard to jurisdictional claims in published maps and institutional affiliations.